Herschel telescope performances and performances degradation

1. Introduction

The Herschel telescope represents the first optical surfaces interacting with the incoming radiation, further detected by the instruments on-board HSO. As such, performances of the telescope will directly affect the quality of observations performed with the instruments. In that philosophy, this note is an attempt to estimate qualitatively and quantitatively the telescope performance degradations from its design parameters as well as its and expected on-ground environments up to its predicted in-flight end-of-life characteristics.

2. Estimation of HSO telescope performances

The telescope design follows the optical parameters described in SCI-PT/08865 (fax from ESA, 17/04/2001). On-sky beam patterns with different model of sources ('top-hat' and gaussian) were presented in SPIRE-RAL-NOT-000118, after modelling diffraction and clipping at M2 edge with ASAP.
The performances, in terms of beam shape quality, of such an electrically large main mirror (at λ=350μm, diameter of M1 ~ 10^4 λ) are difficult to model. Accurate fine sampling (to the order of a few wavelengths) of large M1 and M2 surface areas would be required to simulate with precision the main lobe characteristics (directivity, beamwidth, level and position of the first sidelobes), as well as the wide-angle (i.e. far from boresight, more relevant for straylight) features of the telescope diffraction pattern.
Numerical limitations restrict the range of applications. Example below shows result from computations with Physical Optics (PO, known to describe accurately the main beam zone) applied to Herschel telescope geometry. Even with long intensive computations, only a few arcmins were accessible (see figure 1 below).

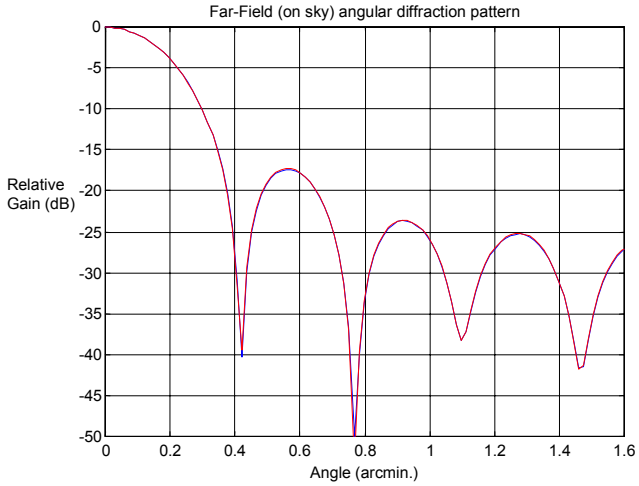

Figure 1: Diffraction pattern, estimated with PO, of Cassegrain telescope with HSO optical parameters.

Alternatively, due to symmetry in the Cassegrain telescope geometry, the far-field telescope pattern was evaluated by rapid (via FFT) computation of the far-field diffraction integral from M1 (effective diameter) aperture field: again after propagation outward from ideal source/feed at SPIRE photometer (centre of FOV) position at the telescope focal plane, including blockage (telescope obscuration) and spillover by/around M2. The simple ideal source used here can be set, from uniform pattern to narrow gaussian-type feed emitter, to different edge tapers (i.e. relative illumination of the telescope mirror edge compare to emitted main beam max). And, in figure 2 below, the case of -3dB (50% of max level at the edge) and -10dB (10% of max level at edge) are considered.

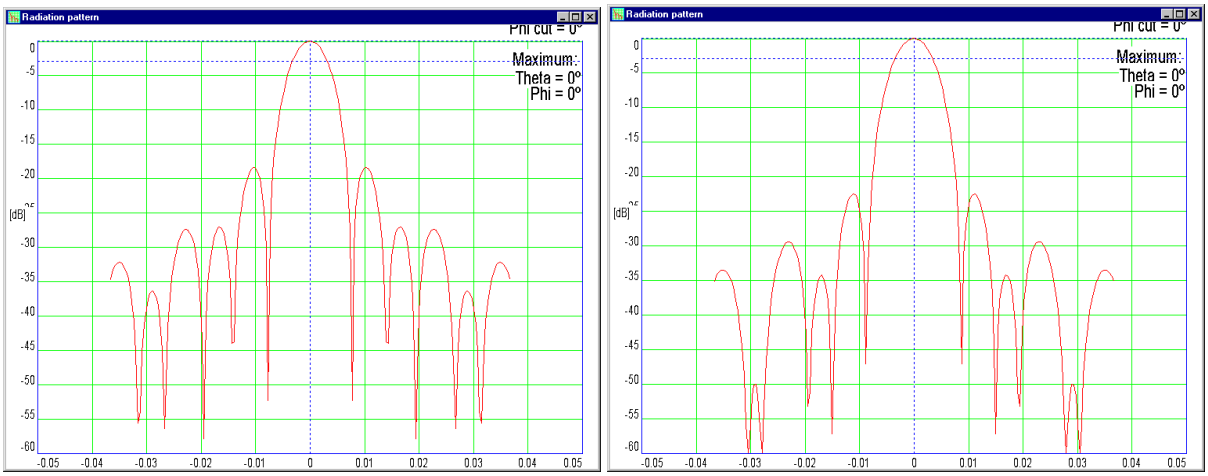

Figure 2: Diffraction patterns (far-field, relative gains) of a Cassegrain telescope with the same optical parameters as for the Herschel telescope. Edge tapers: -3dB (***Left***), -10dB (***Right***). The horizontal axis is the off-axis angle expressed in angular degrees and the wavelength is set to 350 µm.

One can notice the agreement with previous results from ASAP (see SPIRE-RAL-NOT-000118) regarding the position (~ ±0.6/0.8 arcmin), and relative magnitude of the first sidelobes (~ -20dB) although, for the same reasons, only a range limited to about ±2 arcmin can be accurately estimated.
A few more quantitative values, characterising the telescope diffraction patterns, derived from this model have been summarised in the table below for both examples of source illumination level.

Edge taper (dB)	-3	-10
Directivity[1] (dBi)	86.23	88.35
-3 dB beamwidth (arcsec.)	23	24.5
Spillover efficiency (dB)	-3.01	-0.457
Aperture efficiency (dB)	-0.0425	-0.446
Blockage efficiency (dB)	-0.091	-0.129

The spider structure (tripod supporting M2) was neglected; therefore blockage and induced diffraction were not taken into account in the above models. Supplementary diffraction effect from M2 and M1 edges and lateral sunshield were not included (they could be eventually more accessible via GTD/UTD modelling). So these tabulated values should rather represent relative order of magnitude than absolute values. But one can notice the necessary trade-off between the efficient use of the mirror maximum aperture (aperture efficiency) with a rather uniform illumination (leading to a narrower beam on sky) and the need to reduce, by using a 'beam' illumination, the spillover effect (mainly at the pupil M2 in this case), which can also be linked to potential edge diffraction effect and further straylight consideration.

Assuming uniform illumination of the M1 effective diameter, an approximation of the diffraction pattern can be given in term of an analytical Airy pattern with perturbation due to the telescope central obstruction by M2 (ratio taken as 0.05 following SCI-PT/08865) and is displayed in figure 3 below. Although it is an approximation, the main lobe region (figure 3, right) shows good agreement with figure 2 and the wide-angle pattern, through its decreasing asymptotic behaviour (figure 3, left), can be coarsely estimated. The presence of the sunshade on one side would bring asymmetry in the wide-angle pattern via local rise sidelobes level.

[1] A quick way of estimating the directivity D of such a highly directive radio-telescope is:
$D \sim 10\log(2/(1-\cos(\alpha/2))) \sim 20\log(4/\alpha)$ where α is the telescope diffraction cone angle (i.e. $\alpha \sim \lambda/d_{eff}$).

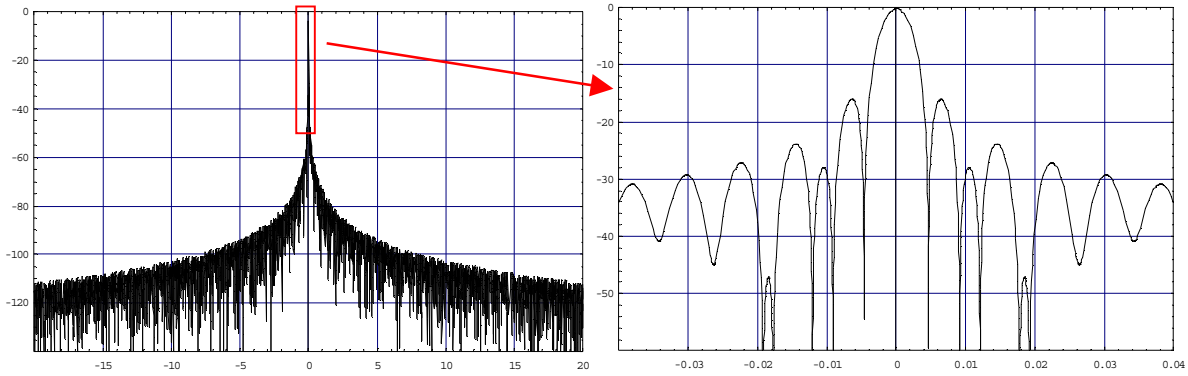

Figure 3: Estimation of the telescope diffraction pattern (relative gain in dB): wide-angle pattern (***Left***) and close-up on the main lobe region (***Right***). Horizontal axis in angular degrees, wavelength set to 350 µm.

Others sources of potential beam quality degradation are the mirror surface defects: roughness and micro-cracks, loss in surface materials and particulate and molecular contamination. For the Herschel telescope, the specified quality of the mirror surface (including polishing) would lead to no significant scattering effect from micro-roughness (<< 1µm rms?) and residual micro-cracks. Loss due to the nature of the upper layer of the mirror surface is difficult to estimate precisely as it is dependent on the material (metals such as Al, Au, Ag, Ni) and quality of the mirror coating material. The fractional power f_L loss from reflection on a metallic surface can be estimated[2] by: $f_L = 2.1\times10^{-4}\sqrt{f(\mathrm{GHz})/\sigma(10^7\,\mathrm{S/m})}$ with σ being the material electric conductivity. At 350µm, this leads to ~0.32% loss per reflection on an aluminium mirror (after taking σ_{Al}~3.65 10^7 S/m at 295K) for example. But this is an estimation at 295K, and at the telescope working temperature, this value may be reduced (depending on the material purity) due to increase of metals conductivity at low temperature. The resulting loss is most likely converted in surface emissivity rather than diffuse background surface scattering. An analysis of the particulate and molecular contamination effects is detailed below.

3. Scattering due to particulate contamination and related telescope performance degradation

At end of life (EOL), an obscuration factor (OR) of 5000ppm for the telescope is expected (see Alcatel Space doc. ref. H-P-1-ASPI-RP-0049, 31/07/01 for the contamination budget). Assessment of the scattering effect from main mirrors (M1 and M2) particulate contamination at this level at a 350µm wavelength was performed with same model as for Planck telescope (same frequency as for Planck-HFI channel, see ESTEC Working paper no2124, Dec. 2000 or ESA Memos ref. 170500/EEA/PDM and ref. 270700/EEA/PDM).

The method can be summarised in the following way: a specifically developed (exposure time dependent) model of contamination is used to define the geometry of the particulate contamination (number and size distribution on the optical surface of interest). A simple Mie model is first used for comparison between geometrical OR and refractive index dependent ('effective') OR based on extinction, scattering and absorption efficiency (via optical cross-section theorem). Then a multiple scattering numerical scheme is applied to evaluate the differential scattering cross-sections (DSCS) for different particle radii in presence of a reflecting surface. Another estimation of the effective OR, now including the optical coupling with the mirror surface, can be derived. The DSCS is then averaged over the previously derived particle size distribution to lead to the surface bi-directional reflection distribution function (BRDF) from particle contamination. The BRDF is finally 'added' (as incoherent

[2] From Goldsmith P., Itoh T., Stephen K., Chapter 7 - *Quasi-optical techniques* in *Handbook of microwave optical components vol.1*, Wiley (1989). This was derived from the relations between emissivity and surface impedance at microwave. A more optical approach using the Hagen-Rubens formula for metals at wavelengths longer than 5-10 µm lead to the same result.

background from surface emitter) to the ideal telescope angular diffraction pattern. The figure 4 below displays the results of such method.

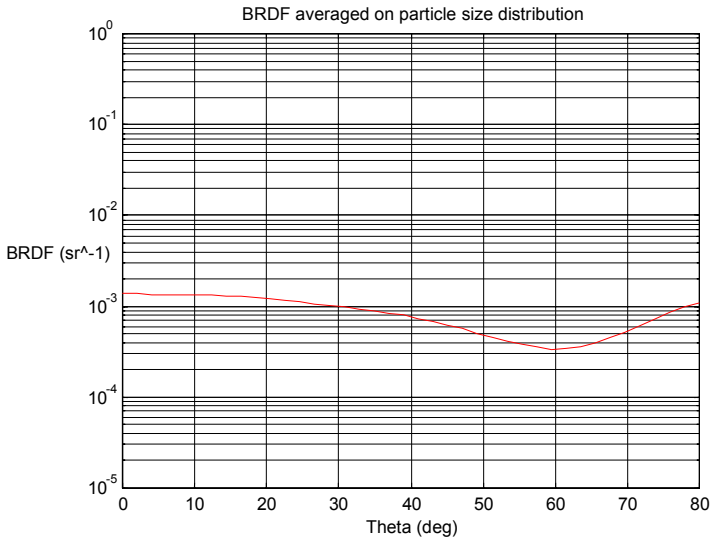

Figure 4: Mirror scattered BRDF for 5000ppm particulate contamination estimated with spherical particles, mixture of materials and normally incident linearly polarised[3] light (at λ=350μm).

Although there is a lack of info concerning the optical properties of the particles at FIR/sub-mm wavelengths, a mixture of absorbing, weakly absorbing and purely refractive materials was used again. In first instance, only particles spherical in shape were considered. Tests were also performed with cylindrical (fibre-like) shape of particles but for the above considered parameters it was found that the BRDF from mixtures of cylindrical particles was close (in level of magnitude and angular distribution) to the one computed for spherical ones (see figure 4 above). Therefore mixing particle shapes, as one would expect dust contaminant to be (small spherical particles, larger fibre ones), would not bring important changes in the estimated contamination-induced BRDF.

To see the effect of the main mirror particulate contamination on the perfect telescope diffraction pattern G_o, the BRDF is included in a 'contaminated' telescope diffraction pattern G_{real} via the following model (see ESA Memo ref. 170500/EEA/PDM):

$$G_{real}(\theta) \approx G_O(\theta) + 10\log(K_O) + 10\log(1 + g_S(\theta)) \text{ with } g_S(\theta) = 2\pi BRDF(\theta)\frac{10^{-\frac{G_o(\theta)}{10}}}{K_O} \text{ and } K_O = e^{-\Phi_{\text{eff}}}$$

For this relatively low level of contamination, it can be approximated that effective OR (Φ_{eff} in the above equation) and the geometric OR are taken as equal, here with 5000ppm EOL value. Although, it should be noticed that the effective OR is actually wavelength dependent: expected to be slightly higher than 0.5% per surface at shortest wavelength (resp. slightly lower at longest wavelengths). Using an average constant value over the angular range of ~10^{-3} sr^{-1} for the BRDF, the above equation is reduced to:

[3] Here only one polarisation is displayed here but the cross-polar component has the same order of magnitude in level and fluctuations with the angle from specular direction. Difference, actually a reduction in BRDF level, appears when the scattering angle gets close to 90deg for the cross-polar term. But at such wide-angle the mirror geometry (curvature) would perturb by further reduction of the BRDF level. Thus, unpolarised radiation would see an average surface BRDF of the same order of magnitude. The shape and magnitude of relative variations of the angular BRDF curve are also strongly wavelength dependent.

$$G_{real}(\theta) \approx G_o(\theta) + 2.210^{-2}.\left(10^{\frac{G_o(\theta)}{10}} - 1\right)$$

In the main peak direction (θ=0, directivity D=G_o(θ=0)~87dBi), the reduction expected by the EOL 5000ppm OR particulate extinction is therefore ~0.022 dB per mirror (too small to be seen on figure 5 below, right). This power loss is partly re-scattered (into the BRDF term) and partly absorbed then re-emitted (increase in surface emissivity). The above model considers only scattering, as the re-emission is several order of magnitudes lower. As quantitative example, one can seek the angular range when the perturbation due to particulate contamination will become higher than the perfect telescope diffraction pattern. For:

$$G_{real}(\theta) - G_o(\theta) = +3dB \quad \Rightarrow \quad G_o(\theta) \approx -21dBi = -108dB$$

So from figure 3 left, one can notice that for θ larger than ~15deg from main peak direction, the diffraction sidelobes will be dominated by scattering effect of the mirror surface particles as illustrated in figure 5 below (using the analytical model for the wide-angle diffraction pattern). Further diffraction effect from non-included objects such as the tripod and the lateral sunshield can also slightly increase the sidelobes level in the ideal pattern in figure 3 (left). The angular range where the pattern is dominated by dust scattering, will then start at an initial larger angle from boresight.

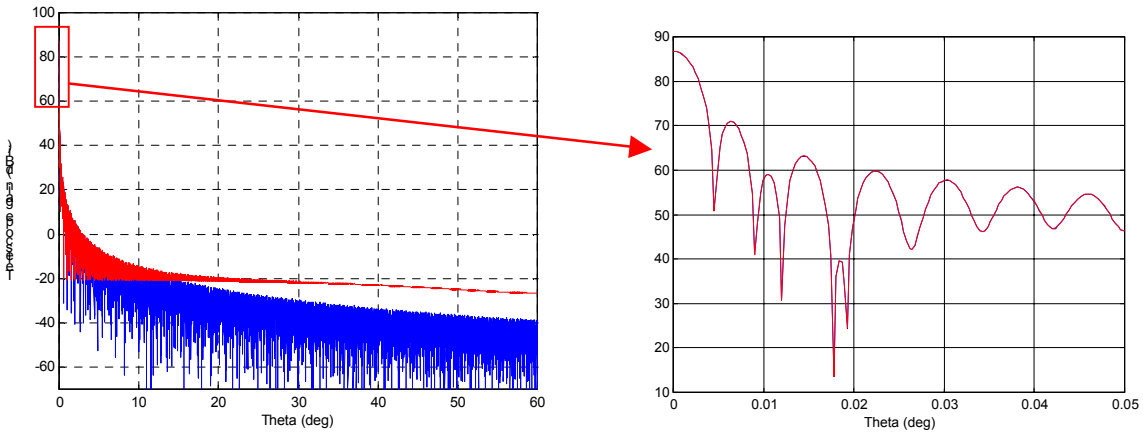

Figure 5: ***Left:*** Wide-angle diffraction pattern of the perfect telescope model (blue) and with scattering effect from EOL level of mirror surface particulate contamination (red). ***Right:*** Close-up on the main peak region.

Molecular contamination is set to an EOL level of 4.10^{-6} g/cm^2 for the Herschel telescope. Assuming light material (density between 0.1 and 1 due organic compounds from on-ground contamination and water/ammonia ice for in-flight one), this level translates into an average thickness of ~10^{-1}µm which is very small compared to the smallest wavelength of interest (λ=350µm). Extrapolating from BRDF data[4] for a molecular 10^{-3}µm thick layer at λ=10.6µm, an estimate for the molecular contaminant contribution to diffuse scattering can be performed. It gives approximate max. values comprised between 10^{-3} and 10^{-4} for the associated BRDF. Therefore no significant increase in surface scattering level would be expected from molecular contamination, as it is slightly smaller than for the particulate one.

However absorption by the molecular layer can increase the mirror surface emissivity. The total increase in emissivity at a mirror surface can be estimated by:

$$\delta e_{total} \approx OR\, e_{particles} + (1 - OR)\, e_{layer} = 5 \times 10^{-3}\, e_{particles} + 0.995 e_{layer}$$

[4] See, for example, Scherr L.M., William Lee W., "*Assessment of condensable molecular and particulate contamination upon optical elements in space system*", SPIE vol.777 Optical System Contamination: Effects, Measurement, Control, 127-137 (1987) and Spyak P.R., Wolfe W.L., ``*Scatter from particulate-contaminated mirrors. Part 3: theory and experiment for dust and λ=10.6µm*", Opt. Eng. **31**(8), 1764-1774 (1992) + ``*Scatter from particulate-contaminated mirrors. Part 4: properties of scatter from dust for visible to far-infrared wavelengths*", Opt. Eng. **31**(8), 1775-1784 (1992).

Assuming an EOL surface transmission[5] T~0.98 per mirror, e_{layer} can be estimated, using the coarse model described in ESA Memo ref. 260700/EEA/PDM, to be around ~1-2% max of the maximum mirror surface value (1-T), leading to e_{layer}~1.10^{-4}-5.10^{-4}. A worst case would consider that all the power loss from the particles to be totally absorbed ('black' particles, no scattering effect) so that $e_{particles}$~1, although a realistic model would be several orders of magnitude lower leading to $e_{particles}$~0.1-0.01. This range of possible values tend to cover the wavelength dependence which is expected (from measurements and theory) to be in $1/\lambda^n$ with n~1-2.
The final variation in surface emissivity δe_{total}, form both combined sources of contamination, would then be expected to be, at max, smaller than 10^{-3} per mirror surface.

[5] From SCI-PT/08865 (fax from ESA, 17/04/2001), the EOL spectral transmission is expected to be >0.96 for the telescope which is taken here as >0.98. This value seems a worst case when compared to all the above mentioned effects but could assume further mirror degradations from a long-term period in space environment (under radiation, debris, …).